



## Active Control of the Bounce and Roll of a Suspension System Using Optimal and Fuzzy Approaches

Ali Sheykhi Kish Khale<sup>1</sup>, Hami Tourajzadeh<sup>2\*</sup>

<sup>1</sup> Department of Mechanical Engineering, University of Guilan, Iran

<sup>2</sup> Associate prof., Mechanical engineering department, Faculty of engineering, Kharazmi University, Tehran, Iran

### ARTICLE INFO

#### Article history:

Received : 16 Apr 2025

Accepted: 25 Sep 2025

Published: 7 Oct 2025

#### Keywords:

Suspension system

Roll control

Bounce control

Fuzzy controller

LQR

### ABSTRACT

Conventional suspension systems exhibit performance limitations when encountering road irregularities and specific surface profiles, often failing to attenuate road-induced disturbances effectively. This functional deficiency reduces ride comfort and compromises vehicle dynamic stability under various driving conditions. In contrast, active suspension systems, utilizing hydraulic or pneumatic actuators in combination with feedback control strategies, have demonstrated a significant potential for disturbance suppression and considerable improvement in ride comfort and vehicle stability. Previous studies have identified that vertical (bounce) and rotational (roll) motions are among the primary factors influencing passenger comfort and vehicle stability in dynamic scenarios. Therefore, controlling these motions is essential to enhance ride quality and handling performance. In this study, a half-car dynamic model equipped with an active suspension system is developed, focusing on controlling bounce and roll motions. All modeling and simulation tasks are conducted within the MATLAB environment, where two control strategies fuzzy control and optimal control are designed and implemented for the active suspension system. Finally, the dynamic performance of these two approaches is compared and analyzed. The simulation results indicate that the optimal control strategy outperforms the fuzzy control method regarding disturbance rejection and overall ride comfort and vehicle stability improvement.

## 1. Introduction

The vehicle suspension system combines springs, dampers, and linkages that connect the chassis to its wheels [1]. In general, suspension systems have traditionally employed the concepts of energy storage and dissipation through springs and dampers [2]. The primary objective of a suspension system is to maximize the frictional contact between the vehicle's tires and the road surface to ensure a safe and comfortable driving experience [3]. Additionally, it guarantees improved ride comfort for passengers.

Active suspension systems employ various strategies by injecting or dissipating energy into or from the system as required. An active suspension system uses a power source to modify the output force in real time continuously. In such systems, controlled forces are applied to the suspension and wheel assembly via hydraulic or electric actuators. An active suspension receives input from road profile information and generates reactive forces in response. The active suspension applies Variable forces at each wheel to continuously adjust the ride and handling characteristics. The key difference between semi-active and fully active suspension systems lies in the presence of an external energy

\*Corresponding Author

Email Address: [Tourajzadeh@khu.ac.ir](mailto:Tourajzadeh@khu.ac.ir)  
<http://doi.org/10.22068/ase.2025.716>

source capable of actively influencing suspension forces[4].

A complete vehicle dynamic model typically consists of seven degrees of freedom: three associated with the vehicle body namely bounce, pitch, and roll and four associated with the vertical displacement of each wheel. Bounce motion is generally defined as the vertical movement of the vehicle's body at its center of gravity. Pitch motion refers to the rotation of the vehicle body about its lateral ( $y$ ) axis. In contrast, roll motion is defined as the vehicle's rotation about its longitudinal ( $x$ ) axis. According to research findings, bounce and pitch motions have a more significant effect on ride comfort than roll motion. Moreover, it has been shown that pitch motion is more perceptible to the human body and, therefore, causes greater discomfort for passengers [4]. As a result, controlling these motions is critically essential for improving ride quality. A half-car model is commonly employed to effectively analyze these dynamics without introducing excessive complexity into the equations of motion, as it sufficiently captures the essential degrees of freedom for bounce and pitch control while simplifying the overall system representation.

A reliable and accurate dynamic model is the foundation for any scientific investigation in this field. Consequently, reviewing the background and progress of suspension system modeling is essential. Lutz et al. [5] recently expanded dynamic modeling approaches in vehicle suspension systems, emphasizing pneumatic tire modeling and proposing a novel model structure. Kayo et al. [6] discussed the dynamics of heavy vehicles from a ride performance design perspective, addressing various aspects of suspension performance. Griffin [7] investigated human perception of vehicle-induced vibration, focusing on measurement and evaluation techniques. Cole David [8] provided a comprehensive review of the impact of heavy commercial vehicles on pavement loading, achieving this through dynamic suspension system modeling. Else et al. [9] highlighted the practical advantages of suspension design through case studies and real-world suspension development examples.

The existing body of research indicates significant efforts in various aspects of conventional vehicle dynamics and suspension system development for passenger cars and commercial vehicles. While extensive studies have been conducted on vehicle roll dynamics, considerably fewer investigations have focused on pitch dynamics. A recent study [10] examined

pitch motion dynamics and the effect of front and rear suspension stiffness configurations in dual-axle heavy vehicles with unlinked suspension systems under a wide range of random road excitations, driving speeds, and braking maneuvers. In that work, well-established vehicle models [11] for dual-axle heavy vehicles with independent and interconnected suspension systems were employed to assess suspension characteristics and performance.

Recent studies on active suspension system control are summarized: Ren and Wu [12] employed PID and neural network control methods. Allen and Liu [13] utilized a variable structure control approach with parameter tuning based on Lyapunov's method. Du and Zhang[14] and Lin and Lian [15] applied fuzzy control strategies.

Both theoretical and experimental results indicate that fuzzy controllers can be powerful tools for controlling systems exhibiting complex or nonlinear motion dynamics [16]. Moreover, using such controllers enhances system robustness against variations in environmental conditions [17]. The proposed fuzzy controller stabilizes the suspension system by effectively rejecting disturbances. In this context, fuzzy control was implemented for a robotic system [18], where the results demonstrated excellent robot motion control and acceptable speed performance. Reference [19] reported implementing a hybrid fuzzy-neural approach to control the motion of a small helicopter, confirming its effectiveness. Subsequently, a similar approach was applied to control the speed of a turbofan engine with unmodeled uncertainties in its dynamic equations [20], which also proved effective.

amshidfar et al. [21] designed an optimal control strategy based on the LQR method to reduce unwanted vibrations in a robotic system. The same approach was applied to a cable-driven robot in [22]. Habibnejad et al. [23] optimized a cable-driven robot using LQR and derived its optimal trajectory in the presence of obstacles and moving boundaries. This optimal control method was then extended to parallel manipulators with flexible joints [24]. Finally, optimal control was employed in [25] for suspended cable robots operating under moving obstacles and parametric uncertainties.

In the present study, an active vehicle suspension system is modeled and simulated based on a half-car dynamic model, focusing on controlling bounce and pitch motions. Using the LQR method, control forces are derived with optimal values to minimize energy consumption. This approach effectively

damps vibrations induced by road excitations by minimizing a defined cost function. All modeling and simulations were performed in the MATLAB environment. Two control strategies fuzzy control and LQR were implemented for the active suspension system, and their performances were compared. The results demonstrate the superior effectiveness of the optimal LQR control method.

## 2. Modeling

To control the pitch and bounce motions of the vehicle, the suspension system is modeled using a half-car dynamic model. In this configuration, the differential motion in the springs and dampers connected to the front and rear wheels generates a rotational motion of the vehicle body known as pitch. As illustrated in Figure 1, the subscript r denotes the rear axle, while f represents the front axle. The input forces are denoted by  $u$ , spring stiffness by  $k_s$ , equivalent tire stiffness by  $k_t$ , and damper damping coefficient by  $c_s$ . The variables  $Z_c$ ,  $Z_s$ ,  $Z_u$ , and  $Z_r$  represent the vertical distances from the smooth road surface, the center of the wheel, the suspension system endpoint, and the vertical displacement of the vehicle's center of gravity.

Like the quarter-car model, this half-car model considers the masses of the suspension components and the vehicle body. Additionally, the vehicle's rotational inertia is included to capture pitch dynamics accurately.

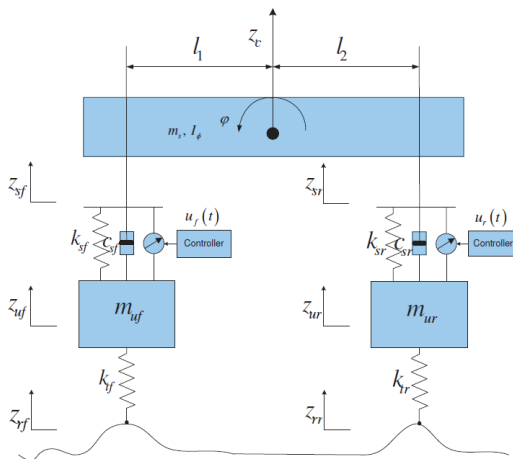


Figure 1 : Schematic of the Half-Car Suspension

Assuming that the vehicle's roll angle  $\phi$  is small, it can be written as:

$$\begin{cases} Z_{sf}(t) = Z_c(t) - l_1\phi(t) \\ Z_{sr}(t) = Z_c(t) + l_2\phi(t) \end{cases} \quad (1)$$

where  $l_1$  and  $l_2$  represent the distances from the rear and front axles to the vehicle's center of

gravity, respectively. Using Newton's second law and considering the static equilibrium point as the reference point for both rotational and linear motion, we proceed to model the motion of this system:

$$\begin{aligned} I_\phi \ddot{\phi} - l_1 k_{sf}(z_{sf} - z_{uf}) - l_1 c_{sf}(\dot{z}_{sf} - \dot{z}_{uf}) + l_2 k_{sr}(z_{sr} - z_{ur}) + l_2 c_{sr}(\dot{z}_{sr} - \dot{z}_{ur}) &= -l_1 u_f + l_2 u_r \\ m_s \ddot{z}_c + k_{sf}(z_{sf} - z_{uf}) + c_{sf}(\dot{z}_{sf} - \dot{z}_{uf}) + k_{sr}(z_{sr} - z_{ur}) + c_{sr}(\dot{z}_{sr} - \dot{z}_{ur}) &= u_f + u_r \\ m_{uf} \ddot{z}_{uf} - k_{sf}(z_{sf} - z_{uf}) - c_{sf}(\dot{z}_{sf} - \dot{z}_{uf}) + k_{tf}(z_{uf} - z_{rf}) &= -u_f \\ m_{ur} \ddot{z}_{ur} - k_{sr}(z_{sr} - z_{ur}) - c_{sr}(\dot{z}_{sr} - \dot{z}_{ur}) + k_{tr}(z_{ur} - z_{rr}) &= -u_r \end{aligned} \quad (2)$$

To find the vertical acceleration of the vehicle at the front and rear axle connection points, by combining equations (1) and (2), we can write:

$$\begin{aligned} \ddot{z}_{sf} &= \ddot{z}_c - l_1 \ddot{\phi} \\ \ddot{z}_{sr} &= \ddot{z}_c + l_2 \ddot{\phi} \\ \ddot{z}_c &= \frac{1}{m_s} (u_f + u_r - k_{sf}(z_{sf} - z_{uf}) - c_{sf}(\dot{z}_{sf} - \dot{z}_{uf}) - k_{sr}(z_{sr} - z_{ur}) - c_{sr}(\dot{z}_{sr} - \dot{z}_{ur})) \\ \ddot{\phi} &= \frac{1}{I_\phi} (l_1 k_{sf}(z_{sf} - z_{uf}) + l_1 c_{sf}(\dot{z}_{sf} - \dot{z}_{uf}) - \dot{z}_{uf}) - l_2 k_{sr}(z_{sr} - z_{ur}) - l_2 c_{sr}(\dot{z}_{sr} - \dot{z}_{ur}) - l_1 u_f + l_2 u_r \end{aligned} \quad (3)$$

Table 1: State-Space Variables

Expression	State Variable	Definition
$z_{sf} - z_{uf}$	$x_1$	Front suspension displacement
$z_{sr} - z_{ur}$	$x_2$	Rear suspension displacement
$z_{uf} - z_{rf}$	$x_3$	Front tire displacement
$z_{ur} - z_{rr}$	$x_4$	Rear tire displacement
$\dot{z}_{sf}$	$x_5$	Front suspension vertical speed
$\dot{z}_{sr}$	$x_6$	Rear suspension vertical speed
$\dot{z}_{uf}$	$x_7$	Front tire vertical speed
$\dot{z}_{ur}$	$x_8$	Rear tire vertical speed

To obtain the state-space form of the dynamic equations, the variables listed in Table 1 are used:

This system has two sets of inputs: 1- the control input  $u$ , which is used to maintain system balance, and 2- the disturbance input  $w$ , which represents road irregularities. The input vector and state variables are as follows:

$$\begin{aligned} \vec{X} &= [x_1 \ x_2 \ x_3 \ x_4 \ x_5 \ x_6 \ x_7 \ x_8]^T \\ \vec{u} &= \begin{bmatrix} u_f \\ u_r \end{bmatrix}, \quad \vec{w} = \begin{bmatrix} \dot{z}_{rf} \\ \dot{z}_{rr} \end{bmatrix} \end{aligned} \tag{4}$$

Then, the state-space form of the dynamic equations will be:

$$\begin{aligned} \dot{\vec{X}} &= A\vec{X} + B\vec{u} + B_1\vec{w} \\ A &= \begin{bmatrix} 0 & 0 & 0 & 0 & 1 & 0 & -1 & 0 \\ 0 & 0 & 0 & 0 & 0 & 1 & 0 & -1 \\ 0 & 0 & 0 & 0 & 0 & 0 & 1 & 0 \\ 0 & 0 & 0 & 0 & 0 & 0 & 0 & 1 \\ -a_1k_{sf} & -a_2k_{sr} & 0 & 0 & -a_1c_{sf} & -a_2c_{sr} & a_1c_{sf} & a_2c_{sr} \\ -a_2k_{sf} & -a_3k_{sr} & 0 & 0 & -a_2c_{sf} & -a_3c_{sr} & -a_2c_{sf} & -a_3c_{sr} \\ \frac{k_{sf}}{m_{uf}} & 0 & \frac{k_{fr}}{m_{uf}} & 0 & \frac{c_{sf}}{m_{uf}} & 0 & \frac{c_{sf}}{m_{uf}} & 0 \\ 0 & \frac{k_{sr}}{m_{ur}} & 0 & \frac{k_{fr}}{m_{ur}} & 0 & \frac{c_{sr}}{m_{ur}} & 0 & \frac{c_{sr}}{m_{ur}} \end{bmatrix} \\ B &= \begin{bmatrix} 0 & 0 & 0 & 0 & a_1 & a_2 & -\frac{1}{m_{uf}} & 0 \\ 0 & 0 & 0 & 0 & a_2 & a_3 & 0 & -\frac{1}{m_{ur}} \end{bmatrix}^T \\ B_1 &= \begin{bmatrix} 0 & 0 & -1 & 0 & 0 & 0 & 0 & 0 \\ 0 & 0 & 0 & -1 & 0 & 0 & 0 & 0 \end{bmatrix}^T \end{aligned} \tag{5}$$

Now, using the above model, we can proceed with the vehicle control.

### 3.1. Fuzzy Controller

Fuzzy controllers demonstrate acceptable efficiency and performance in controlling the motion of complex systems and executing specific maneuvers. One common design approach for fuzzy controllers involves decomposing the system's complex behaviors into several motions within its operational range. After designing appropriate control algorithms for each segment, their corresponding actions can be combined.

This study uses a fuzzy controller to determine suitable control forces to achieve the desired control objectives while maintaining good robustness against external disturbances. This controller is formulated based on a set of if-then rules in the following form:

$$\begin{aligned} \text{If } l_i \text{ is } A \text{ and } \dot{l}_i \text{ is } B, \\ \text{then } u_i \text{ is } C \end{aligned} \tag{13}$$

In the continuation, the AND and OR operators are defined as follows:

$$\begin{aligned} \mu_{A \cup B} &= \text{Max}(\mu_A(u), \mu_B(u)) \\ \mu_{A \cap B} &= \text{Min}(\mu_A(u), \mu_B(u)) \end{aligned} \tag{14, 15}$$

In the proposed controller, Mamdani-type fuzzy logic and the centroid defuzzification method were employed. In the first stage, the fuzzy controller performs the fuzzification process after receiving the inputs. Then, based on the equation (13) and the Mamdani implication method, the membership functions are combined using a fuzzy operator. In the next step, the values of the membership functions are aggregated using the union operator according to equation (14), and the outputs are then defuzzified.

The inputs to the fuzzy system were selected as the error and the derivative of the error from the desired value at a given time. The membership functions for these inputs were considered as Gaussian functions. The position and velocity errors were categorized into five membership functions: [-2, -1, 0, +1, +2], with the variation range for both position and velocity errors set to [-1, 1]. This represents a general case, and to adjust the range of position and velocity errors, a scaling factor can be applied to the system error.

For the fuzzy system's output which represents the required control force to guide the robot along a specified path the membership functions were also chosen as Gaussian functions based on the Mamdani method. Finally, Figure 2 presents a graphical representation of the membership functions for both the system's inputs and output.

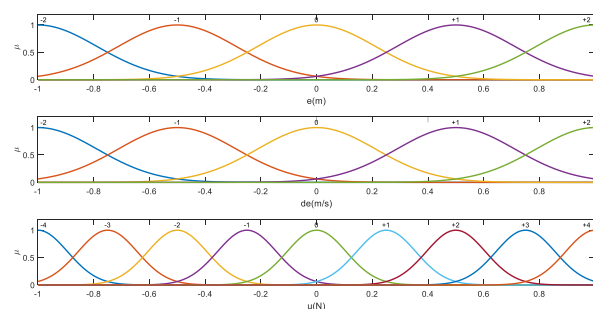


Figure 2 : Membership functions of the input and output of the Mamdani fuzzy system

Finally, the fuzzy rule set for extracting the appropriate control force was selected as follows:

**Table 1 : Selected Fuzzy Rule Set**

Number	Fuzzy rules			
1	-2	-2	+4	
2	-2	-1	+3	
3	-2	0	+2	
4	-2	+1	+1	
5	-2	+2	0	
6	-1	-2	+3	
7	-1	-1	+2	
8	If "e" is	and "de" is	then "u" is	+1
9	-1	+1	0	
10	-1	+2	-1	
11	0	-2	+2	
12	0	-1	+1	
13	0	0	0	
14	0	+1	-1	
15	0	+2	-2	
16	+1	-2	+1	
17	+1	-1	0	
18	+1	0	-1	
19	+1	+1	-2	
20	+1	+2	-3	
21	+2	-2	0	
22	+2	-1	-1	
23	+2	0	-2	
24	+2	+1	-3	
25	+2	+2	-4	

**3-2- Optimal LQR Controller**

The objective of the LQR control method is to determine the optimal control inputs  $u^*$  that, when applied to the system described by equation (11), not only stabilize the system and satisfy the defined constraints but also minimize the cost function defined in equation (16). Additionally, the system's state variables are driven to converge to zero with minimal control effort.

$$J(X, u, t) = \frac{1}{2} X^T(t_f) H X(t_f) + \frac{1}{2} \int_{t_0}^{t_f} [X^T Q X + u^T R u] dt \tag{16}$$

In this context, H and Q are symmetric positive definite weighting matrices, and R is a strictly positive definite weighting matrix. These matrices R and Q can be expressed as follows:

$$R = \begin{bmatrix} \frac{1}{u_{1max}^2} & 0 \\ 0 & \frac{1}{u_{2max}^2} \end{bmatrix} \tag{17}$$

$$Q = \begin{bmatrix} \frac{1}{X_{1max}^2} & 0 & \dots & 0 \\ 0 & \frac{1}{X_{2max}^2} & \vdots & 0 \\ \vdots & \vdots & \ddots & \vdots \\ 0 & \dots & \dots & \frac{1}{X_{8max}^2} \end{bmatrix}_{8 \times 8}$$

The general form of the control input calculated from equation 18 is:

$$u^* = -R^{-1} B^T K X \tag{18}$$

In this method, K represents the Lagrangian multipliers (or feedback gain matrix) obtained by solving the algebraic Riccati equation given in equation (19). This equation is solved from the initial simulation time to the final time using the initial values of the system's state variables.

$$-KA - A^T K - Q + KBR^{-1}B^T K = 0 \tag{19}$$

To solve this equation in MATLAB, the care function is defined. The system equations in the presence of the controller are as follows:

$$\dot{Z}_1 = C_1 \vec{X} + D_1 \vec{u}^* \tag{20}$$

Where  $u^*$  is the optimal control input, which is calculated according to the method described above.

**4- Simulation**

All simulations were conducted using the values provided in Table 2.

**Table 2 : Vehicle Parameters**

Parameter	Symbol	Unit	Value
Vehicle Mass	M <sub>1</sub>	Kg	1300
Suspension Mass	M <sub>2</sub>	Kg	150
Suspension Spring Stiffness	k <sub>1</sub>	N/m	20000
Tire Equivalent Spring Stiffness	k <sub>2</sub>	N/m	150000
Suspension Damping Coefficient	b <sub>1</sub>	N.s/m	1500
Tire Equivalent Damping Coefficient	b <sub>2</sub>	N.s/m	7020
Distance from Center of Gravity to Rear Suspension	l <sub>2</sub>	m	1.5
Distance from Center of Gravity to Front Suspension	l <sub>1</sub>	m	1
Vehicle Moment of Inertia	J	Kg.m <sup>2</sup>	2000

4-1- Dynamic Model Simulation

Using the dynamic model presented in equation (5), the vehicle's dynamic behavior during bounce and pitch motions is simulated. In this problem, road disturbances (W) are modeled using a step input, representing a vehicle encountering a speed bump or similar road irregularity in real-world conditions. The transfer function responses corresponding to the bounce and pitch motions concerning a unit step input were obtained to simulate the system dynamics without applying any control. For this purpose, the Step command in MATLAB was used. The outputs of this simulation are shown in the following figures.

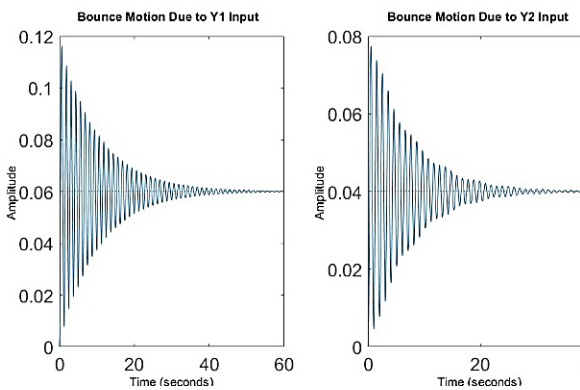


Figure 2 : The response of the transfer function for pitch motion to step inputs for Y1 (front wheel disturbance) and Y2 (rear wheel disturbance)

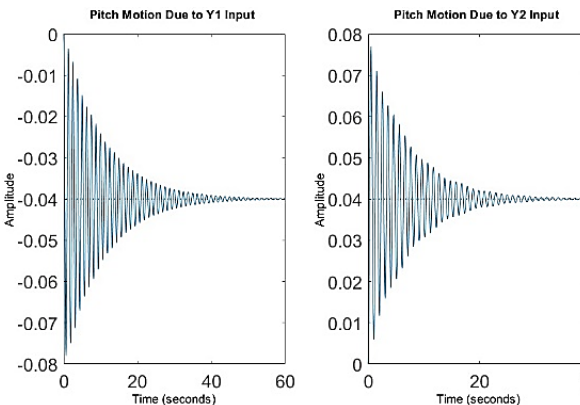


Figure 3 : The response of the transfer function for roll motion to step inputs for Y1 (front wheel disturbance) and Y2 (rear wheel disturbance)

As observed, the vibrations induced by this excitation reach an acceptable level of damping over approximately 50 seconds. During this period, the system continuously vibrates, causing passengers discomfort and adversely affecting the vehicle's handling and steering responsiveness.

It is also evident that in the pitch motion, the amplitude of the vibrations resulting from the front

wheel disturbance is greater than that caused by an equivalent disturbance at the rear wheel. This is due to the shorter distance between the front wheel and the vehicle's center of gravity. Naturally, if the pitch motion is evaluated relative to the center of gravity, the closer the disturbance occurs to the center of gravity, the larger the resulting pitch angle for a disturbance of equal magnitude.

This behavior confirms the accuracy of the modeling approach using the half-car dynamic model, as it appropriately captures the effects of the vehicle geometry and suspension characteristics on the dynamic response.

4.2 Control

This study aims to suppress vibrations caused by disturbances such as road bumps while maintaining the vehicle's stability. To achieve this, a controller was designed using feedback from the system outputs, aiming for an overshoot of less than 5% for  $x_1 - x_2$  and a settling time shorter than 5 seconds.

For example, when the simulated vehicle model is subjected to a step input disturbance of 10 centimeters, the body oscillates within  $\pm 5$  millimeters and stabilizes within 5 seconds.

The fuzzy controller is simulated using the membership functions and control rules presented in the previous section.

Next, to implement the LQR controller, the gain matrix was selected as follows:

$$R = \begin{bmatrix} 1 & 0 \\ 0 & 1 \end{bmatrix}$$

$$Q = 10^{10} \times \text{diag}([1 \ 1 \ 1 \ 1 \ 0.04 \ 0.04 \ 0.04 \ 0.04]) \tag{21}$$

Where Q is a diagonal matrix with its central diagonal values specified.

An initial condition error and an external disturbance were applied to the system to evaluate the system's performance better. The initial conditions in this case are defined as follows:

Both wheels simultaneously encounter a speed bump, with the front wheel displaced by 10 centimeters and the rear wheel displaced by 5 centimeters.

Additionally, the disturbance profile considered for both the front and rear wheels is a step wave, starting at 1.5 seconds and lasting for 0.1 seconds, as illustrated below:

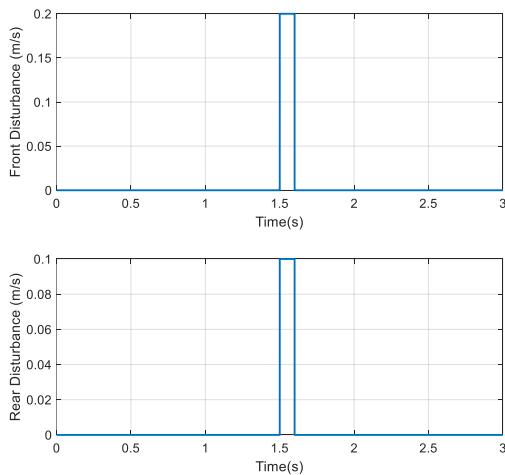


**Figure 4 : A representation of the disturbance profile considered for the front and rear wheels**

The results obtained from the simulation of the system under the specified conditions and the implementation of the controllers are as follows:

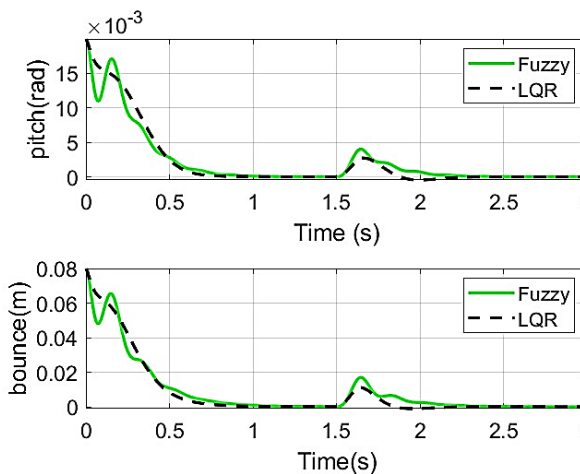


**Figure 5 : Comparison of bounce and roll movements in fuzzy PD controllers and LQR**

As shown in Figure 5, the LQR controller follows a smoother trajectory than the fuzzy controller when encountering both the initial condition error and the external disturbance and converges to the desired stable point in a completely uniform manner without any additional oscillations. This indicates the superior optimality of the LQR controller over the applied fuzzy controller.

Moreover, the LQR controller reaches full convergence while passing through smaller local maxima, demonstrating higher robustness against external disturbances. Although both controllers were able to gradually suppress the effect of the speed bump over time, the LQR controller

exhibited better performance in more rapidly reducing the oscillations.

The control forces applied by the controllers are as follows:

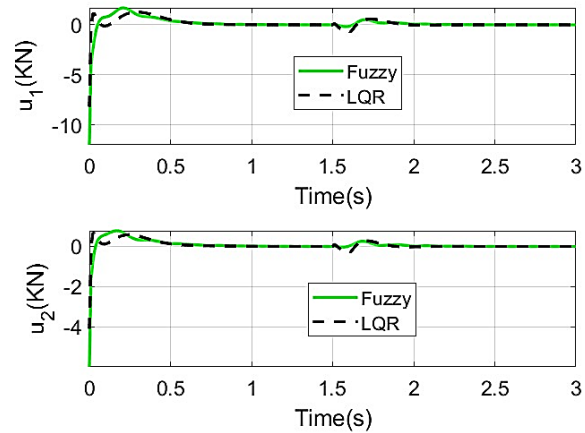


**Figure 6 : Comparison of control forces for the front axle ( $u_1$ ) and rear axle ( $u_2$ ) in fuzzy PD and LQR controllers.**

As shown in Figure 6, the absolute value of the control force in the LQR controller starts from a lower magnitude than that in the fuzzy controller, indicating higher optimality. Both controllers maintained a smooth and uniform force profile throughout the trajectory, remaining within a reasonable range.

When the external disturbance was applied, the LQR controller demonstrated higher agility than the fuzzy controller within the same time frame, which contributed to better suppression of the applied disturbance.

It is also noteworthy that the integral of the cost function throughout the simulation was  $4.46 \times 10^7$  for the uncontrolled system,  $2.90 \times 10^7$  when using the fuzzy controller, and  $1.92 \times 10^7$  for the LQR controller further confirming the superior performance and efficiency of the LQR controller over the fuzzy controller.

### 5- Conclusion

In this study, the dynamic half-car model was selected for the suspension system and modeled accordingly. Two control methods, Fuzzy Logic and linear quadratic regulator (LQR), were employed to control the active suspension system. All modeling and simulations were performed in the MATLAB environment, and the mathematical model's validity was confirmed.

In the mathematical model simulation without applying any control, it was observed that the vibrations induced by a disturbance with an amplitude of 0.1 reached an acceptable level of damping after approximately 50 seconds. During

this period, the system remained vibratory, causing discomfort for the passengers and negatively affecting the vehicle's handling performance.

Both designed controllers successfully achieved their objectives in the mathematical simulations, stabilizing the system within a desirable timeframe. However, based on the observations, the suspension system's bounce and pitch motions exhibited up to 25% lower vibrations under the LQR controller compared to the fuzzy controller, thereby offering passengers a smoother and more comfortable ride.

Furthermore, the absolute value of the control force in the LQR controller started from a value up to 25% lower than that of the fuzzy controller, indicating higher optimality and efficiency for the LQR method.

**List of symbols**

Symbol	Description
$U$	Control input force
$M_1$	Vehicle body mass
$M_2$	Suspension system mass
$k_s$	Suspension spring stiffness
$k_t$	Equivalent tire stiffness
$C_s$	Suspension damper damping coefficient
$J$	Vehicle moment of inertia
$l_1$	Distance from the center of gravity to the front suspension
$l_2$	Distance from the center of gravity to the rear suspension
$K_p$	Proportional gain
$K_i$	Integral gain
$K_d$	Derivative gain
$R$	LQR weighting matrix
$Q$	LQR weighting matrix
$H$	Weighting matrix

**Reference**

[1] Y. Liu, "Recent innovations in vehicle suspension systems," *Recent Patents on Mechanical Engineering*, vol. 1, no. 3, pp. 206-210, 2008.

[2] W. A. Smith and N. Zhang, "Recent developments in passive interconnected vehicle suspension," *Frontiers of Mechanical Engineering in China*, vol. 5, no. 1, pp. 1-18, 2010.

[3] D. Maher, "Combined time and frequency domain approaches to the operational identification of vehicle suspension systems," Dublin City University, 2011.

[4] W. C. T. Burke, "Large force range mechanically adjustable dampers for heavy vehicle applications," Virginia Tech, 2010.

[5] A. Lutz, J. Rauh, and W. Reinalter, "Developments in vehicle dynamics and the tire model performance test," *Vehicle System Dynamics*, vol. 45, no. S1, pp. 7-19, 2007.

[6] D. Cao, S. Rakheja, and C.-Y. Su, "Heavy vehicle pitch dynamics and suspension tuning. Part I: unconnected suspension," *Vehicle System Dynamics*, vol. 46, no. 10, pp. 931-953, 2008.

[7] M. J. Griffin, "Discomfort from feeling vehicle vibration," *Vehicle System Dynamics*, vol. 45, no. 7-8, pp. 679-698, 2007.

[8] D. J. Cole, "Fundamental issues in suspension design for heavy road vehicles," *Vehicle System Dynamics*, vol. 35, no. 4-5, pp. 319-360, 2001.

[9] P. S. Els, N. J. Theron, P. E. Uys, and M. J. Thoresson, "The ride comfort vs. handling compromise for off-road vehicles," *Journal of Terramechanics*, vol. 44, no. 4, pp. 303-317, 2007.

[10] D. Cao, S. Rakheja, and C. Su, "Pitch plane analysis of a twin-gas-chamber strut suspension," *Proceedings of the Institution of Mechanical Engineers, Part D: Journal of Automobile Engineering*, vol. 222, no. 8, pp. 1313-1335, 2008.

[11] A. Odhams and D. Cebon, "An analysis of ride coupling in automobile suspensions," *Proceedings of the institution of mechanical engineers, Part D: Journal of Automobile Engineering*, vol. 220, no. 8, pp. 1041-1061, 2006.

[12] J.-C. Renn and T.-H. Wu, "Modeling and control of a new 1/4T servo-hydraulic vehicle active suspension system," *Journal of Marine Science and Technology*, vol. 15, no. 3, p. 12, 2007.

[13] A. Alleyne and R. Liu, "A simplified approach to force control for electro-hydraulic systems," *Control Engineering Practice*, vol. 8, no. 12, pp. 1347-1356, 2000.

[14] H. Du and N. Zhang, "Fuzzy control for nonlinear uncertain electrohydraulic active suspensions with input constraint," *IEEE Transactions on Fuzzy systems*, vol. 17, no. 2, pp. 343-356, 2008.

[15] J. Lin and R.-J. Lian, "Intelligent control of active suspension systems," *IEEE*

- Transactions on industrial electronics*, vol. 58, no. 2, pp. 618-628, 2010.
- [16] A. Derdiyok, B. Soysal, F. Arslan, Y. Ozoglu, and M. Garip, "An adaptive compensator for a vehicle driven by DC motors," *Journal of the Franklin Institute*, vol. 342, no. 3, pp. 273-283, 2005.
- [17] D. Chwa, "Fuzzy adaptive tracking control of wheeled mobile robots with state-dependent kinematic and dynamic disturbances," *IEEE transactions on Fuzzy Systems*, vol. 20, no. 3, pp. 587-593, 2011.
- [18] L. Vermeiren, A. Dequidt, M. Afroun, and T.-M. Guerra, "Motion control of planar parallel robot using the fuzzy descriptor system approach," *ISA transactions*, vol. 51, no. 5, pp. 596-608, 2012.
- [19] N. Al-Falooji and M. Abbod, "Helicopter control using fuzzy logic and narma-l2 techniques," 2020.
- [20] F. Lu, Z. Yan, J. Tang, J. Huang, X. Qiu, and Y. Gao, "Iterative learning NARMA-L2 control for turbofan engine with dynamic uncertainty in flight envelope," *Proceedings of the Institution of Mechanical Engineers, Part G: Journal of Aerospace Engineering*, vol. 236, no. 7, pp. 1282-1294, 2022.
- [21] H. Jamshidifar, B. Fidan, G. Gungor, and A. Khajepour, "Adaptive vibration control of a flexible cable driven parallel robot," *IFAC-PapersOnLine*, vol. 48, no. 3, pp. 1302-1307, 2015.
- [22] M. Rushton and A. Khajepour, "Optimal actuator placement for vibration control of a planar cable-driven robotic manipulator," in *2016 American Control Conference (ACC)*, 2016: IEEE, pp. 3020-3025.
- [23] M. Korayem, A. Zehfroosh, H. Tourajizadeh, and S. Manteghi, "Optimal motion planning of non-linear dynamic systems in the presence of obstacles and moving boundaries using SDRE: application on cable-suspended robot," *Nonlinear Dynamics*, vol. 76, no. 2, pp. 1423-1441, 2014.
- [24] S. Kilicaslan, "Tracking control of elastic joint parallel robots via state-dependent Riccati equation," *Turkish Journal of Electrical Engineering and Computer Sciences*, vol. 23, no. 2, pp. 522-538, 2015.
- [25] A. Behboodi and S. Salehi, "SDRE controller for motion design of cable-suspended robot with uncertainties and moving obstacles," in *IOP Conference Series: Materials Science and Engineering*, 2017, vol. 248, no. 1: IOP Publishing, p. 012031.